



# Impact of High-Volume GNSS Radio Occultation Data on the Navy's Global Numerical Weather Prediction

Hui W. Christophersen<sup>1</sup>, Ben Ruston<sup>2</sup>, and Dan Tyndall<sup>1</sup>

<sup>1</sup>Naval Research Laboratory Marine Meteorology Division, Monterey, CA, USA

5 <sup>2</sup>Joint Center for Satellite Data Assimilation (JCSDA) at the University Corporation Atmospheric Research (UCAR), Boulder, CO, USA

*Correspondence to:* Hui W. Christophersen (hui.w.christophersen.civ@us.navy.mil)

**Abstract.** This study assesses the impact of assimilating high-volume Radio Occultation (RO) data from the RO modeling experiment (ROMEX) on the Navy's global operational Naval Global Environment Model (NAVGENM). A series of observation  
10 system experiments were conducted, including a control run, a standard assimilation of all ROMEX data, and two sensitivity tests: one with an empirical bias correction and another with a modified refractivity coefficient. Results indicate that while the standard assimilation of ROMEX data improved free-tropospheric moisture forecasts, it amplified existing model biases in temperature and geopotential height, leading to forecast degradation. In contrast, both sensitivity experiments led to substantial improvements in forecast skill. The empirical bias correction method proved most effective, yielding consistent forecast  
15 improvements across temperature, moisture, and geopotential height. A Forecast Sensitivity to Observation Impact (FSOI) analysis confirmed the positive contribution of all ROMEX missions, with Spire missions providing the largest total impact and COSMIC-2 showing the highest per-observation effectiveness. The findings underscore that an adjustment to the current treatment of the observation was critical to fully realize the benefits of the large volume of RO observations. While the empirical bias correction delivers the greatest forecast improvements, it may obscure and reinforce persistent model biases. The refractivity  
20 coefficient adjustment offers an alternative that preserves the unbiased nature of RO observations.

## 1 Introduction and Motivation

Radio Occultation (RO) is a remote sensing technique that exploits the bending of radio signals as they traverse the Earth's atmosphere to retrieve highly accurate profiles of temperature, pressure, and humidity. RO tracks signals transmitted by Global Navigation Satellite Systems (GNSS) such as Global Positioning System (GPS), GLONASS, Galileo, and BeiDou, and received  
25 by a low-Earth orbit (LEO) satellite. As the GNSS satellite sets (or rises) behind the Earth's limb from the perspective of the LEO satellite, the radio signals are refracted due to changes in atmospheric density. By analyzing the bending angle of these signals, we can reconstruct the atmospheric refractive index profile, which is then used to derive profiles of temperature, pressure, and humidity at vertical resolutions of 0.5 km in lower troposphere (Kursinski et al., 1997). The current GNSS-RO constellation gathers measurements with near complete global coverage daily (Anthes et al. 2024).

30 RO plays a significant role for Numerical Weather Prediction (NWP) systems due to its ability to provide highly accurate and stable atmospheric profiles that are crucial for initializing weather models (Healy and Thépaut, 2006; Aparicio and Deblonde, 2008; Cucurull and Derber, 2008; Ruston and Healy, 2020). Unlike many traditional observations, RO data is largely unaffected by cloud cover and precipitation, making it particularly valuable in data-sparse regions and challenging weather conditions. As a stable, all-weather data source, RO is a critical component of the global observing system that significantly improves forecast  
35 accuracy, especially in the stratosphere and upper troposphere.



Harnisch et al. (2013) used an ensemble data assimilation (EDA) framework to assess how GNSS RO impact scales with observation number in ECMWF. Their result suggested GNSS RO impact increases with observation count without saturation (up to 128,000 profiles/day), with ~16,000 profiles delivering about half the total impact under assumed error characteristics. Using an Observing System Simulation Experiment (OSSE), Cucurull et al. (2018) found that increasing the number of  
40 assimilated RO profiles has the potential to significantly benefit NWP systems, improving both anomaly correlation and 72-h forecast skill with the addition of 12,000 COSMIC-2 refractivity profiles. Privé et al. (2022) further concluded that information saturation remains unmet despite the addition of 100,000 RO soundings per day. In response to these findings, the International Radio Occultation Working Group (IROWG) under the Coordination Group for Meteorological Satellites (CGMS) of the World Meteorological Organization (WMO) established the RO modelling experiment (ROMEX) (Anthes et al., 2024). ROMEX is a  
45 collaborative effort among various data providers, data processing centers, and NWP centers to evaluate the impact of high-volume RO data on NWP. The Naval Research Laboratory (NRL) is one of many NWP centers to independently evaluate the impact of ROMEX data on the Navy's global NWP.

This study is organized as follows: Section 2 describes the ROMEX data, the NWP and data assimilation system, and experiment designs. Section 3 presents the impacts of ROMEX data. The last section summarizes the findings and concluding remarks.

## 50 **2 Methodology**

### **2.1 ROMEX**

The ROMEX dataset consists of RO observations collected over a three-month period from September through November 2022. During this time, observations from all available RO missions were aggregated to create a dense global dataset. On average, approximately 30,000–40,000 RO profiles per day were obtained, representing roughly three times the number of RO  
55 observations currently used in operational NWP systems. The dataset includes observations from both traditional government satellite missions and newer commercial RO providers. Table 1 lists all the RO missions that provide data as part of the ROMEX dataset.

ROMEX includes neutral-atmosphere profiles of bending angle and refractivity, covering the troposphere, stratosphere, and lower mesosphere. These variables are directly assimilated in many NWP DA systems and provide high-vertical-resolution  
60 information with global coverage and minimal bias. Further details on ROMEX can be found in Anthes et al. (2024).

### **2.2 NAVGEM and its Data Assimilation System**

The operational Naval Global Environment Model (NAVGEM; Hogan et al., 2014) at T681L60 (~19 km horizontal resolution with a model top at 0.04 hPa) was employed for this study. NAVGEM's data assimilation (DA) system is a dual-space strong constraint four-dimensional variational (4DVar) hybrid system (Kuhl et al., 2013; Rosmond & Xu, 2006; Daley & Barker, 2000).  
65 The DA system routinely ingests about 4 million observations for each 6-h DA cycle (Stone et al., 2020; Frolov et al., 2020). These observations include conventional sources such as radiosondes, aircraft, buoys, and ships, as well as satellite-derived atmospheric motion vectors and ocean surface winds. Additionally, satellite radiance data from various microwave (MW) and infrared (IR) sensors are used, along with ozone retrievals, GNSS RO and ground-based zenith total delay (Christoffersen et al., 2023). The operational DA system also routinely ingests government procured commercial RO data from Spire and PlanetIQ.  
70 GNSS RO bending angles are assimilated using a 1D variational approach that utilizes forward, tangent linear and adjoint models from the EUMETSAT Radio Occultation Processing Package (ROPP; Culverwell et al., 2015). No vertical thinning is applied to the RO bending angle assimilation. Details of the quality control procedures followed are provided in Bowler et al. (2026), while the observation error specification is described in Ruston and Healy (2020)



### 2.3 Experiment Design

75 Two sets of experiments were conducted (Table 1). In the first set, the control run excludes RO data from commercial providers (Spire, GeoOptics, PlanetIQ), and Chinese providers (Tianmu, Yunyao, and FengYun series) (romex\_cntl). The ROMEX experiment (romex) assimilates the full ROMEX datasets. An additional experiment, romex\_noro, was also performed in which all RO observations were excluded from assimilation. The second set consists of two modified ROMEX sensitivity experiments: one employing a simple empirical bias correction scheme applied to the observation (romex\_bc), and the other adjusting the dry refractivity coefficient in the forward operator used to compute refractivity (romex\_n1).

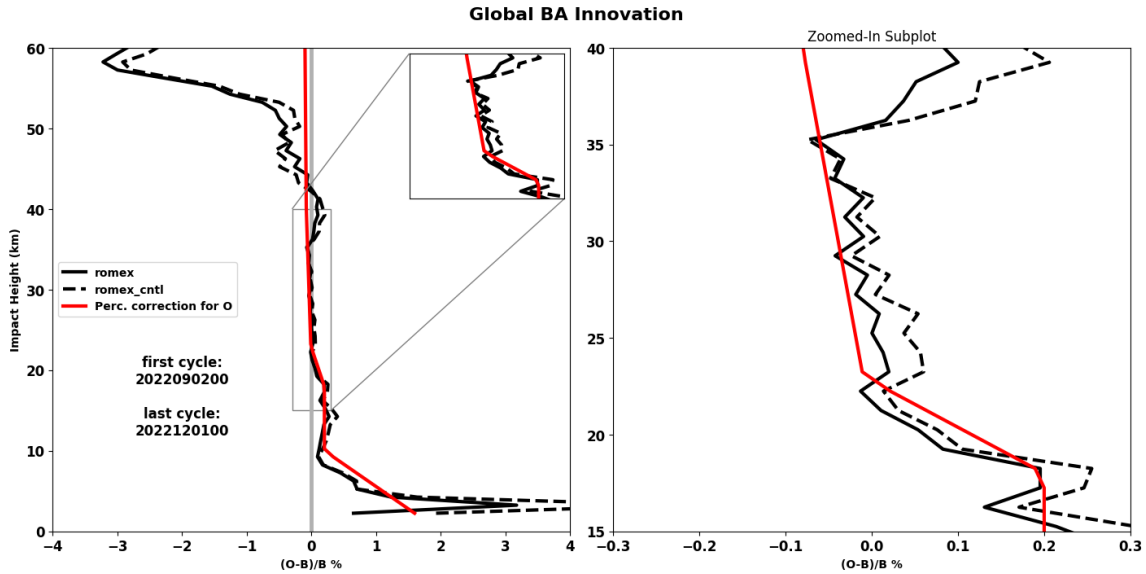
Table 1: Description of experiments carried out in this study.

	Exp. Name	Description	RO missions	Duration
Exp. Set I	romex_cntl	Assimilate RO as in operational NAVGEM but exclude data sources from commercial and Chinese providers	<i>MetOp, Sentinel-6, COSMIC-2, Kompsat-5, PAZ, TerraSAR-X, TanDEM-X</i>	September - November 2022
	romex	Assimilate all RO data from ROMEX	Those in the control run plus <i>Spire, PlanetIQ, GeoOptics, FY3x, Yunyao, Tianmu</i>	
	romex_noro	No RO assimilation	None	
Exp. Set II	romex_n1	Same as “romex” except the first dry refractivity coefficient is decreased by 0.1%	Same as “romex”	
	romex_bc	Same as “romex” except an empirical bias correction is applied to the observations	Same as “romex”	

Specifically, the empirical bias correction was derived from the whole 3-month ROMEX background normalized innovations, where innovation is defined as the difference between the satellite observations (**O**) and the model's first guess (**B**) from either the romex or romex\_cntl experiment. A simple bias correction model was constructed using linear interpolation between several hinge points in the vertical. For each bending angle observation, a small correction ( $y'$ ), expressed as a function of impact height ( $h$ ) in Eq. (1), was applied.

$$y' = \begin{cases} \text{linearly ramped to 2\%,} & h \leq 10 \text{ km} \\ 0.2\%, & 10 < h < 18 \text{ km} \\ \text{linearly varies from } -0.01\% \text{ to } 0.2\%, & 18 \leq h < 23 \text{ km} \\ \text{linearly varies from } -0.08\% \text{ to } -0.01\%, & 23 \leq h < 40 \text{ km} \\ 0.1\%, & h \geq 40 \text{ km} \end{cases} \quad (1)$$

Fig. 1 illustrates this empirical bias correction model. Although a large negative bias in the innovations is apparent above an impact height of 40 km, we applied only a small constant correction to these observations. The observations at these altitudes have relatively large prescribed observation errors (Ruston and Healy, 2020), hence they are expected to have a limited impact on the analysis. The empirical model primarily focuses on corrections in the core region (zoomed-in panel in Fig. 1) and in the atmospheric boundary layer.



95 **Fig. 1: Global bending angle normalized innovation for the ROMEX experiment (“romex”) and the control experiment (“romex\_cntl”) as a function of impact height. The empirical bias correction model derived from all ROMEX RO bending angle observations is also shown (red lines). The right panel shows a zoomed-in view of the left panel for impact heights between 15 and 40 km.**

In romex\_n1 experiment, we performed a sensitivity study on the forward simulation of atmospheric refractivity ( $N$ ). This was done by reducing the first refractivity coefficient ( $k_1$ ) by 0.1%, changing its value from the standard 77.643 K hPa<sup>-1</sup> to  $k_1^*=77.565$

100 K hPa<sup>-1</sup>. The refractivity ( $N$ ) is then calculated using the formula established by Smith and Weintraub (1953):

$$N = k_1^* \left( \frac{P_d}{T} \right) + k_2 \left( \frac{P_v}{T} \right) + k_3 \left( \frac{P_v}{T^2} \right) \quad (2)$$

where  $P_d$  and  $P_v$  represents the partial pressure of dry air and water vapor, respectively, within a volume of moist air.  $T$  denotes the temperature in Kelvin. The standard coefficient values used in the ROPP are  $k_1=77.643$  K hPa<sup>-1</sup>,  $k_2=77.643$  K hPa<sup>-1</sup>, and  $k_3=3.73 \cdot 10^5$  K<sup>2</sup> hPa<sup>-1</sup> (Culverwell et al. 2015).

105 All experiments were initiated using the operational NAVGEM satellite bias correction coefficients and restart files valid at 0000 UTC on 1 September 2022. All experiments end at 0000 UTC on 2 December 2022. As such, all the DA cycles from 1 September to 30 November 2022 except the initial cold start cycle were included in the statistical analysis.

### 3 Results

#### 3.1 Bending angle innovation characteristics

110 We first examined the characteristics of innovation profiles in all the experiments. Figure 2 presents the global bending angle innovations normalized by error estimates as a function of impact height for the three ROMEX experiment from 0600 UTC 1 September to 0000 UTC 1 October 2022. This analysis is a critical first step in diagnosing systematic biases between the observations and the model.

115 Overall, the normalized mean innovation ( $O-B$ )/ $B$  remains close to zero between approximately 10 km and 35 km, indicating that the model background fields are largely unbiased relative to the observations within this altitude range. However, noticeable differences among the experiments appear between roughly 35-50 km. At these higher altitudes, the mean innovations from the romex\_bc experiment exhibit a larger positive bias compared to the romex and romex\_n1 experiments, suggesting that the



empirical observation bias correction may introduce a systematic bias in this region. In contrast, the romex\_n1 experiment produces mean innovations that remain closer to those of the romex experiment while showing a slightly reduced bias, particularly above 35 km, but also from 10-35 km (Fig.2, inset in the left panel) a critical region as the observation errors are lowest in this region. In the lower troposphere (below approximately 10 km), all experiments exhibit larger positive innovations and increased variability. This behavior is expected due to the stronger influence of moisture, multipath effects, and representativeness errors in RO observations at low altitudes. Although differences between experiments are present, they are relatively small compared to the overall variability in this region.

The normalized innovation standard deviation  $(\mathbf{O}-\mathbf{B})/\sigma_o$  ( $\sigma_o$  represents the observation error) provides an indication of consistency between observation and instrument error specifications within the data assimilation system. Ideally, when properly normalized, these values should remain close to zero mean with unity variance. The results (Fig. 2, right panel) show generally small variability throughout most of the vertical column, suggesting that the observation error specification is broadly consistent across experiments. However, romex\_bc shows slightly larger deviations between approximately 35 and 45 km, implying that the correction may introduce additional noise or misrepresentation of background uncertainty. In general, the romex experiment shows larger innovation standard deviations below 15 km compared with both romex\_bc and romex\_n1.

Overall, this suggests that use of the ROMEX observations with the current ROPP forward operator may accentuate small systematic biases, a finding that will further be substantiated in our evaluation of impact on the analysis and short-range forecasts. To remove the small bias and ensure successful assimilation, we processed the data using either an empirical bias correction or a more physically-based refractivity coefficient adjustment.

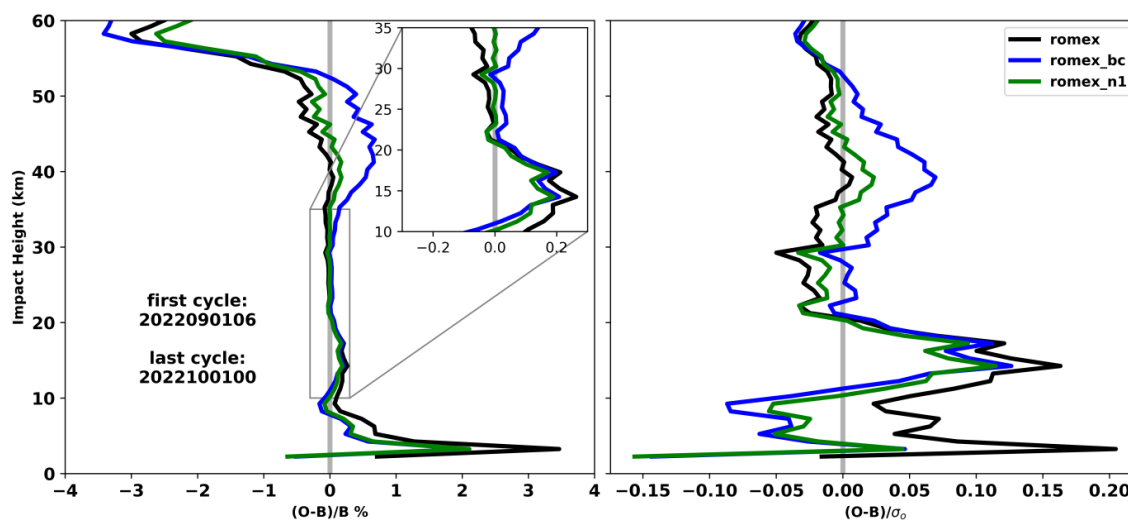


Fig. 2: Global bending angle innovation normalized (a) by the background (B) and (b) by the observation error ( $\sigma_o$ ) for the ROMEX experiment (“romex”), bias-corrected ROMEX experiment (“romex\_bc”), and adjusting refractivity coefficient ROMEX experiment (“romex\_n1”) as a function of impact height.

### 3.2 Impact on analysis and short-range forecasts

We also investigated the respective impact from the assimilation of ROMEX observations on model background by examining how well the model first guesses fit to independent data such as radiosondes, commonly also known as fit-to-observations (fit2obs) (e.g. Duncan et al. 2022). Background fit2obs assesses how well observations improve or degrade short-range (6-h)



forecasts. A reduction in the standard deviation of these background departures indicates that the model's background forecast  
145 has become more accurate. This improvement is a direct result of assimilating the new ROMEX observations. We evaluated the  
fit2obs analysis on global radiosonde observations from September to November 2022. The performance is evaluated for four  
radiosonde variables: temperature (T), pseudo relative humidity (PRH), and the U- and V- components of wind. PRH is an  
analysis moisture variable used in the NAVGEM DA system, computed as specific humidity scaled by the saturation specific  
humidity using the background temperature at the observation location and time (Dee & Da Silva, 2003).

150 Figure 3 illustrates the impact of the different experiment configurations on the model's background forecast, showing the  
normalized standard deviation of the background departure from radiosonde observations across various pressure levels. The  
romex\_bc and romex\_n1 experiments consistently demonstrate the most significant forecast improvements, with their  
normalized standard deviations staying well below the 100% baseline for most of the atmosphere. This indicates a marked  
reduction in forecast error, particularly for temperature at nearly all pressure levels and for PRH between 300 and 700 hPa. Both  
155 experiments also show better fit to radiosonde winds at tropospheric levels between 250 and 850 hPa, but the improvements for  
upper-level radiosonde winds above 200 hPa are smaller in the romex\_bc and romex\_n1 experiment compared to the romex  
experiment.

The romex experiment shows more mixed improvements. Benefit is found in the model background for temperature at 100–400  
hPa, PRH at 400–925 hPa, and winds at pressure levels below ~250 hPa. Outside these vertical regions, the romex experiment  
160 exhibits mostly neutral impacts or slight degradations in the background fields. The degradation in the PRH above ~250 hPa may  
be attributed to the use of PRH as analysis variables in the DA system (Baker et al., 2017), or simply model stratospheric  
moisture error.

It is worth noting that the romex\_noro experiment, which excludes the assimilation of RO data, consistently results in a negative  
impact on the forecast accuracy. It shows significant degradation across all variables, as expected, confirming the critical positive  
165 contribution of RO data to the model's predictive skill.

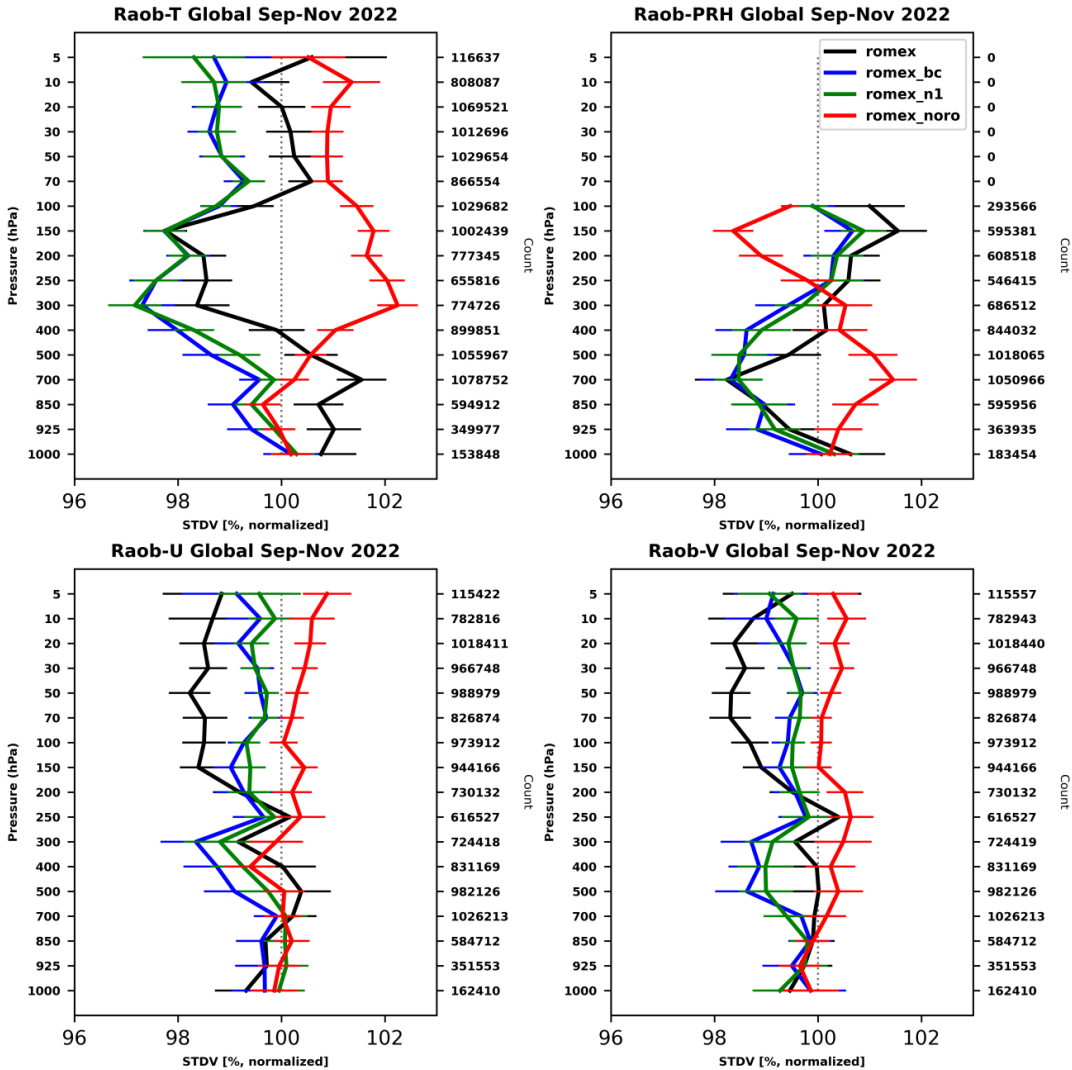


Fig. 3. Change in standard deviation of observed minus background for radiosondes temperature, pseudo relative humidity (PRH), and zonal and meridional wind relative to the control experiment for ROMEX (“romex”), bias-corrected romex (“romex\_bc”), adjusting the first refractivity coefficient ROMEX experiment (“romex\_n1”), and the one without RO data (“romex\_noro”) experiment from September to November 2022. The number of observations is indicated on the vertical axis to the right, and the horizontal bars represent the 95% significance level.

The impact of ROMEX observation assimilation is further examined by the forecast sensitivity to observation impact (FSOI; Langland and Baker, 2004). FSOI quantifies the direct contribution of each ROMEX observation to reducing the 24-h forecast error. Larger FSOI values here indicate larger beneficial impact, meaning that the observation contributed to improving the forecast.

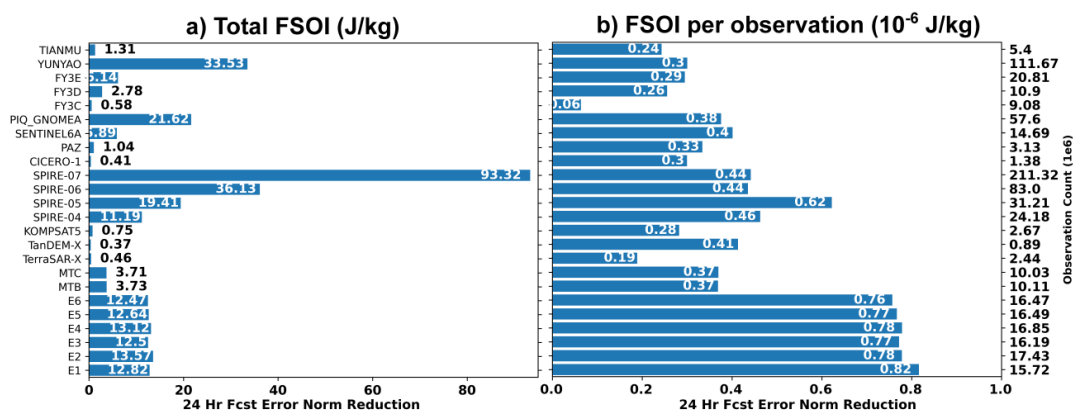
Fig. 4 depicts both the cumulative impact of all RO observations as well as per-observation FSOI from the romex\_n1 experiment. All ROMEX missions contribute positively to reducing forecast error. Note the right-hand y-axis of Fig. 4b contains the total observation counts over the study period. The Spire missions are grouped into families by satellite generation using



180 receiver ID ranges: Spire-04 (99-102), -05 (103-117), -06 (118-125) and Spire-07 (126-169). The groupings correspond to different Spire satellite generations (mission families) with similar instrument characteristics. Spire-07 provides the largest contribution. Overall, the Spire observations are cumulatively highest in number, and subsequently account for the largest total beneficial impact. Among the Chinese providers, YUNYAO contributes the largest total beneficial impact. COSMIC-2 missions also provide a substantial beneficial contribution to the forecast system.

185 When the impact is normalized by the number of observations (Fig. 4b), the per-observation FSOI is relatively consistent across the different RO instruments. The FY3C is on the lowest side of per observation impact, and the bulk of RO instruments lie in an approximate range of 0.3 – 0.45. This indicates comparable effectiveness at the individual observation level for the NAVDAS-AR system which uses an RO receiver agnostic quality control and error model. However, the six COSMIC-2 receivers exhibit the largest per-observation FSOI among all the missions considered. Fig. 4 shows the results of the romex\_n1 experiment, but

190 the FSOI characteristics for other romex experiments are similar. All experiments provide consistent evidence that assimilating the ROMEX data is beneficial for NWP.



195 **Fig. 4: (a) Total forecast sensitivity to observation impact (FSOI, J/kg) and (b) per observation FSOI for all the ROMEX missions from September to November 2022 from the romex\_n1 experiment. Spire instrument receiver IDs are grouped as follows: Spire 04 (99–102), Spire 05 (103–117), Spire 06 (118–125), and Spire 07 (126–169). E1-6 are COSMIC-2 missions.**

### 3.3 Impact on medium-range forecasts

To assess medium-range forecast skill, we used our ROMEX-enhanced data assimilation and forecasting system to evaluate the percentage reduction in root-mean-square error (RMSE) for key variables (geopotential height, temperature, and specific humidity) relative to the control experiment, verified against ECMWF analyses. These forecast RMSE differences are evaluated as a function of forecast lead time and pressure for three latitude bands: Southern Hemisphere (SH, 20°–80°S), tropics (TR, 20°S–20°N), and Northern Hemisphere (NH, 20°–80°N).

200

Fig. 5 from top to bottom depicts the RMSE reduction (%) for geopotential height forecasts in the romex, romex\_bc, and romex\_n1 experiments relative to the romex\_cntl experiment, verified against ECMWF analyses. Fig. 6 complements this analysis by showing vertical profiles of the mean geopotential height analysis differences relative to ECMWF for each experiment and region. The romex experiment, the upper panels in Fig. 5, exhibits statistically significant degradation (>3%) of the geopotential height forecast skill across most regions and forecast lead times, particularly in the mid- to upper troposphere. In the TR and NH, this degradation increases with forecast lead time, suggesting a systematic positive bias that grows during the forecast integration. This behavior is consistent with the analysis statistics shown in Fig. 6. All experiments exhibit a generally positive geopotential height bias relative to ECMWF analyses; however, the romex experiment further amplifies this positive

205

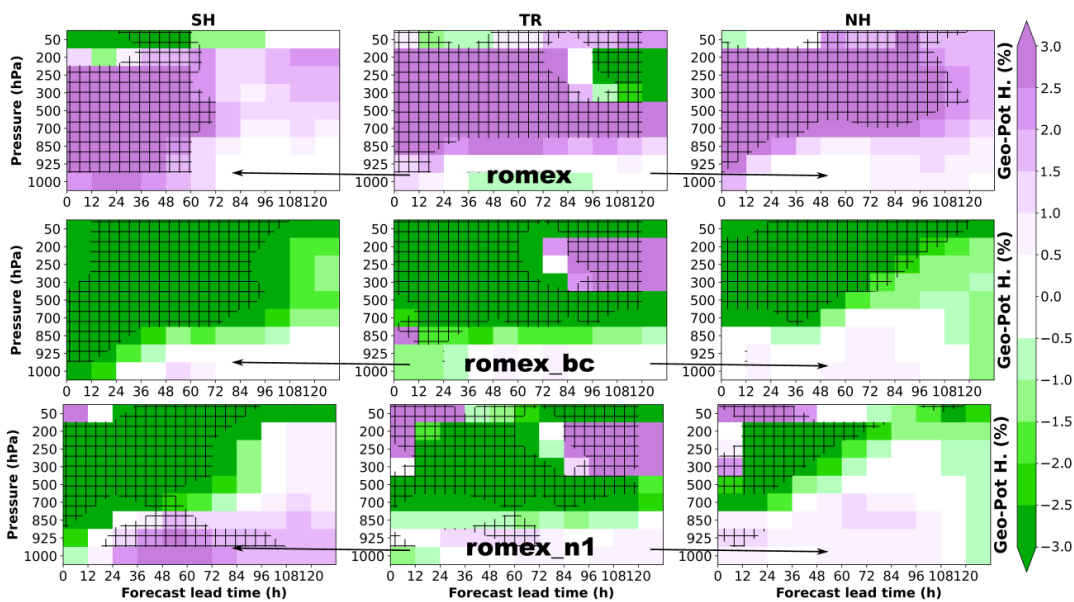


210 bias relative to the control run at the analysis time across nearly all regions and throughout much of the troposphere and lower stratosphere. Further, the lower panels of Fig. 6 show that the romex experiment degrades the analysis against the control, with both the romex\_n1 and romex\_bc in general providing benefit by this measure. The bias in the romex experiment is particularly pronounced in the mid-troposphere of the NH, indicating that the standard assimilation in romex experiment that increases the RO impact by sheer volume of observations, introduces a persistent overestimation of geopotential height.

215 Applying the empirical bias correction (romex\_bc) substantially alters this influence of the RO observations on the analysis and forecast. In Fig. 5, the widespread forecast degradation seen in the romex experiment is largely reduced or reversed, especially in the troposphere. Improvements of more than 3% dominate many regions, particularly in the SH and TR, and the statistically significant areas indicate that these improvements are robust over large portions of the forecast period. Fig. 6 further confirms this shift: romex\_bc reduces the positive geopotential height bias at the analysis time relative to the control run across most  
220 pressure levels and regions. This reduction in analysis bias likely contributes to the improved forecast skill seen in the RMSE statistics. By nature, the empirical bias correction would not differentiate between a persistent bias in the observation or background forecast. Therefore, the romex\_bc would also bring the observation closer to a systematic model bias and indeed shows the best result with respect to the romex\_cntl.

The romex\_n1 experiment yielded a net positive impact, performing better than the romex experiment but falling short of the  
225 gains seen in romex\_bc. Notably, while the response was largely positive, it did introduce a few isolated negative impacts. In Fig. 5, the geopotential height differences are generally smaller in magnitude compared to romex, and broadly more consistent with the romex\_bc experiment. The romex\_n1 experiment does introduce a mix of improvements and degradations depending on region, pressure level and forecast lead time. Slight degradation was observed in the SH at pressures of 850 hPa and higher, at early lead times in the NH, and at 50 hPa, particularly within the first 48 hours. The vertical profiles in Fig.6 support this  
230 interpretation: romex\_n1 reduces the analysis bias relative to the control experiment, but increases this analysis bias above 200 hPa in TR and NH. This suggests that the modified refractivity coefficient used in romex\_n1 can help demonstrate a positive impact of ROMEX observations on analyses and forecasts, but may not be sufficient to fully offset large model bias. This is consistent with the idea that an adjustment of the refractivity coefficient used in the romex\_n1 experiment acts directly on the observation and can be used to diagnose model biases.

235 Regional differences are also evident. The SH shows relatively larger sensitivity to the experiment configuration, especially in the upper troposphere and lower stratosphere. This likely reflects the greater relative influence of satellite observations in observational data-sparse regions. In contrast, the TR exhibit strong vertical gradients in the geopotential height differences, with the largest discrepancies occurring in the mid-troposphere. The NH displays more moderate changes, likely due to the stronger constraint provided by dense conventional observations.



240

Fig. 5: Percentage change in root-mean-square-error (RMSE) reduction for geopotential height forecasts in the “romex”, “romex\_bc”, and “romex\_n1” experiments relative to the control, verified against ECMWF analyses for September–November 2022. Forecast RMSE is computed every 12 hours for the control and comparison experiment at three distinct regions: Southern Hemisphere (SH, 20°–80°S), tropics (TR, 20°S–20°N), and Northern Hemisphere (NH, 20°–80°N). Green shading indicates improved forecast skill from the assimilation of ROMEX observations, while purple shading signifies degraded skill. Hatched areas denote impacts that are statistically significant at the 95% confidence level.

245

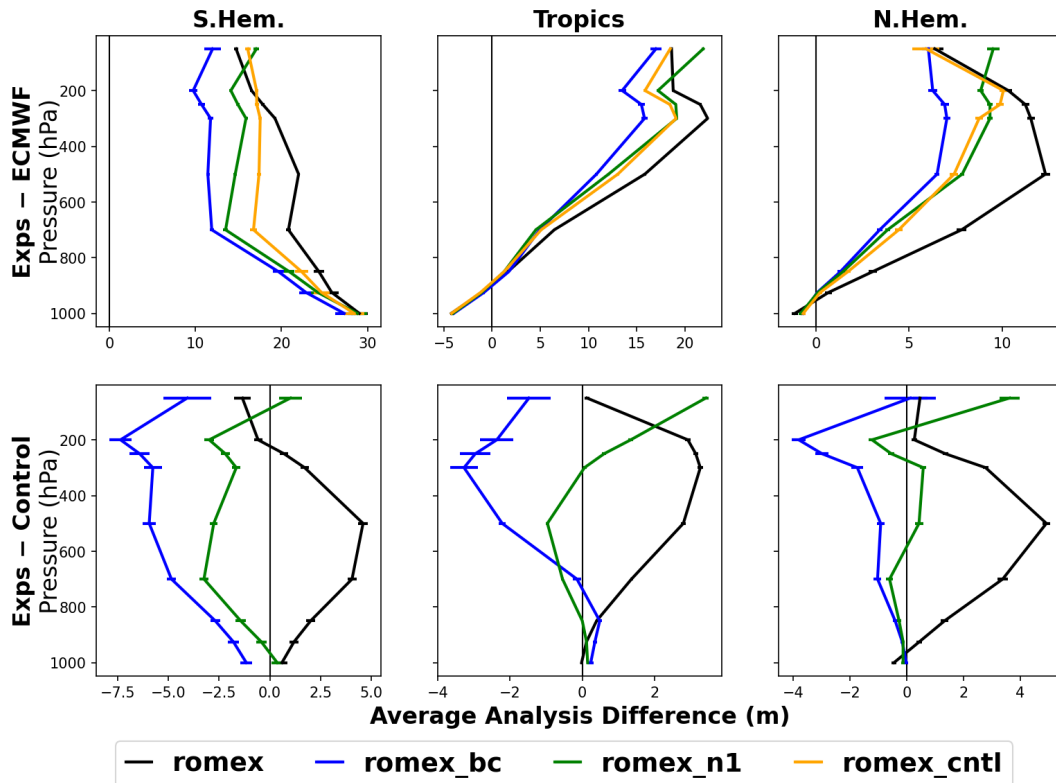


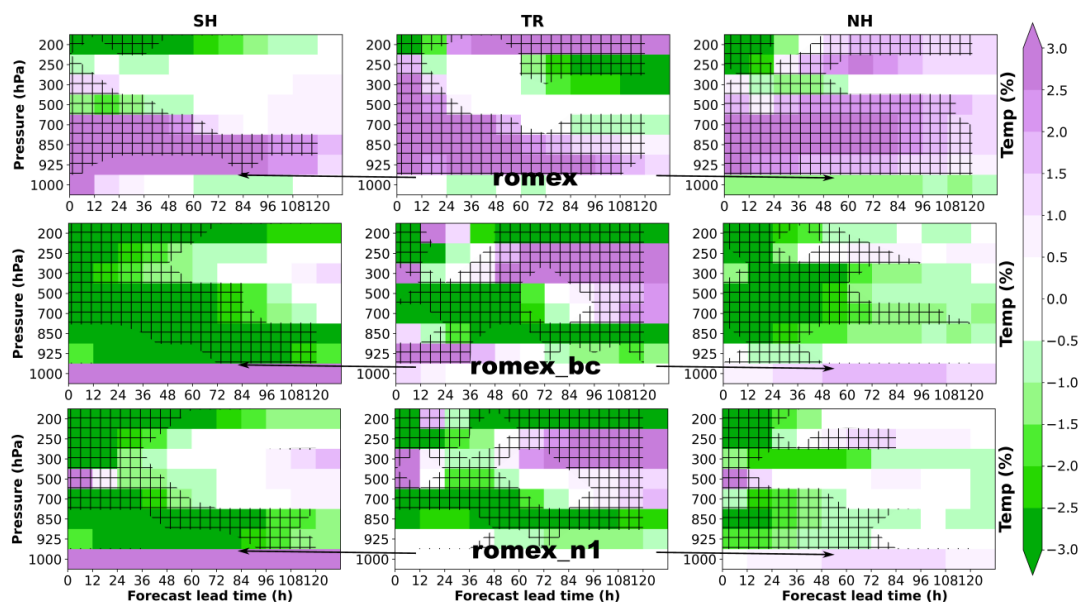
Fig. 6: (Top) Mean geopotential height analysis bias (units: m) between each romex experiment (romex, romex\_bc, romex\_n1) and ECMWF analyses, (bottom) and between each romex experiment and the control run. Statistics are computed using analyses initialized at 0000 UTC and 1200 UTC from 1 September to 30 November for the southern hemisphere (SH), tropics (TR) and northern hemisphere (NH). Error bars indicate the 95% confidence interval estimated using a two-sample t-test accounting for lag-1 autocorrelation (Wilks 2011, pp. 145-149). Note that the x-axis range in the top panel differs from that in the bottom panel.

Temperature results show a similar relationship between analysis bias and forecast impact. The romex experiment shows statistically significant degradation in temperature forecasts throughout much of the troposphere (upper panels Fig. 7). Only limited improvements are observed during the first 24 hours of forecast lead time above 250 hPa across all regions. The analysis statistics shown in Fig. 8 indicate that, with respect to ECMWF, the NAVGEM temperature analysis exhibits a pronounced warm bias in the lower troposphere and a cold bias aloft. The romex experiment further amplifies these existing temperature biases over the romex\_cntl throughout much of the tropospheric column, consistent with the degraded forecast performance.

In contrast, romex\_bc substantially improves temperature forecast skill. As shown in the middle row of Fig. 7, romex\_bc produces a positive forecast impact exceeding 3% in many regions, particularly in the Southern and Northern Hemispheres from 925 hPa up to the mid-upper troposphere for lead times extending to 3–4 days. In the TR, however, the impact is more mixed, with statistically significant improvements primarily confined to a narrower layer between approximately 400 and 850 hPa for lead times up to three days. The strong positive impact in the NH gradually diminishes beyond two days of forecast lead time. At the analysis time, Fig. 8 shows that romex\_bc effectively reduces the lower-tropospheric warm bias in the Southern and Northern Hemispheres and produces a similar bias reduction within the narrow tropical layer where forecast improvements are observed.



The romex\_n1 experiment exhibits a broadly similar pattern of forecast improvement compared to romex\_bc, although the magnitude of the temperature forecast improvement is slightly smaller. Figure 8 confirms that the adjustment to the temperature analysis bias in romex\_n1 follows a similar vertical structure to romex\_bc but with reduced amplitude.



270

Fig. 7: Same as Fig. 5, but for temperature.

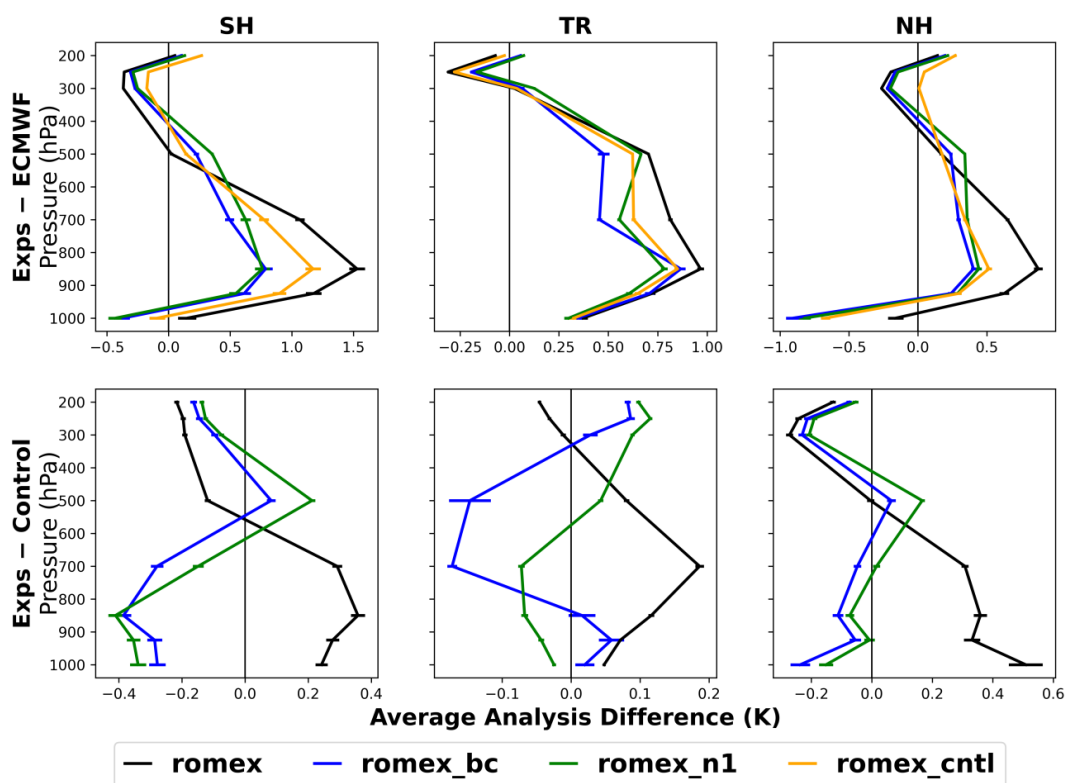




**Fig. 8: Same as Fig. 6, but for temperature (unit: K).**

275 Moisture forecasts exhibit a different response to the ROMEX assimilation. Unlike the widespread degradations seen in  
geopotential height and temperature forecasts, the romex experiment produces positive improvement in moisture forecasts. Fig. 9  
shows that the romex experiment leads to positive forecast impact for precipitable water above ~850 hPa extending to upper  
troposphere. The improvement is approximately 2-3% at the initial forecast time and gradually decreases after two days for the  
SH and NH, while remaining evident through much of the 5-day forecast period in the TR. However, the romex experiment also  
280 introduces substantial degradation in precipitable water forecasts within boundary layer (below 900 hPa).

To better understand these forecasts impacts, Fig. 10 examines the corresponding analysis differences using specific humidity,  
which provides finer vertical resolution than precipitable water. The control experiment exhibits a dry-moist-dry bias structure  
relative to the ECMWF analyses from the surface to the upper troposphere. The romex experiment increases the positive  
moisture bias relative to the romex\_cntl experiment, with the largest contribution near 900hPa. As a result, the assimilation of  
285 ROMEX partially corrects the dry bias in the free troposphere above ~850hPa, leading to an improved moisture forecast in that  
region. However, this correction overcompensates in the lower troposphere and boundary layer, contributing to forecast  
degradation at these levels.

The romex\_bc and romex\_n1 exhibit broadly similar significant positive impact on moisture forecasts. Both experiments  
produce statistically significant improvements in precipitable forecasts up to ~400 hPa for lead time extending beyond 2-3 days  
290 (Fig. 9), although slight forecast degradation is evident above this level. In contrast to the romex experiment, both romex\_bc and  
romex\_n1 experiments reduce the moisture analysis bias relative to the control (Fig. 10), with the largest adjustment around 700  
hPa. This more balanced analysis moisture bias correction likely contributes to the improved forecast performance compared  
with the standard romex experiment.

Overall, these results demonstrate that the treatment of ROMEX observations using an empirical bias correction or by adjusting  
295 the refractivity coefficient strongly influences the impact that RO data on both analysis bias and forecast skill. The standard  
romex experiment tends to amplify existing model biases in geopotential height and temperature, leading to degraded forecast  
performance despite some improvements in free-tropospheric moisture forecasts. Applying an empirical bias correction  
(romex\_bc) effectively reduces negative impacts with respect to ECMWF, the control and radiosonde observation and yields the  
most consistent forecast improvements; however, the romex\_bc approach will not allow the observations to address model bias.

300 The modified refractivity formulation used in romex\_n1 largely provides positive impact on analysis, forecasts and fit to  
radiosonde though not to the degree found with romex\_bc. In addition, the romex\_n1 is applied more directly to the observation  
and can be used to diagnose and mitigate model biases.

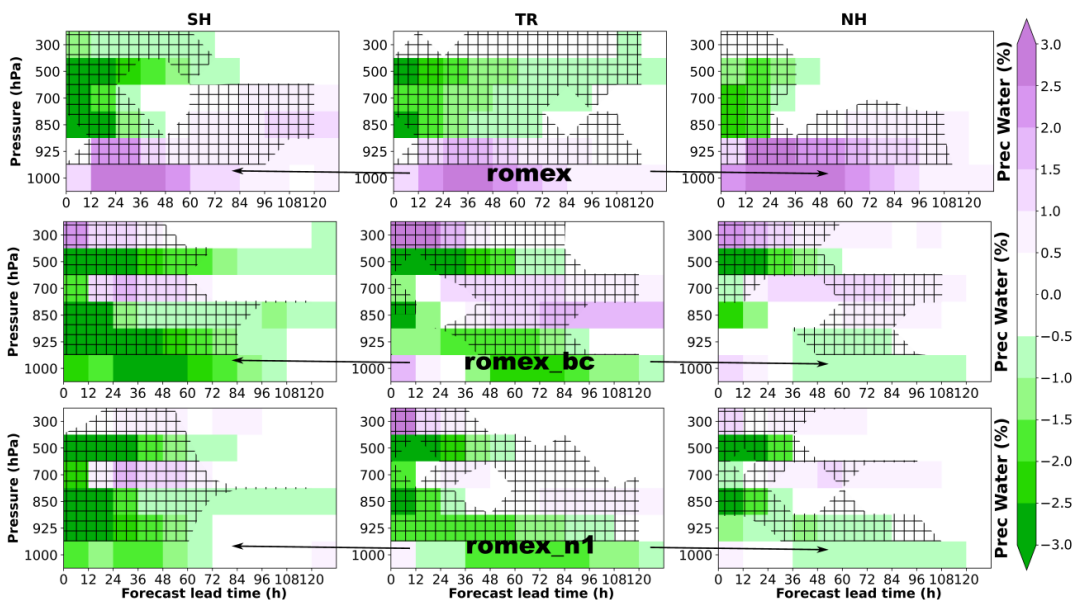
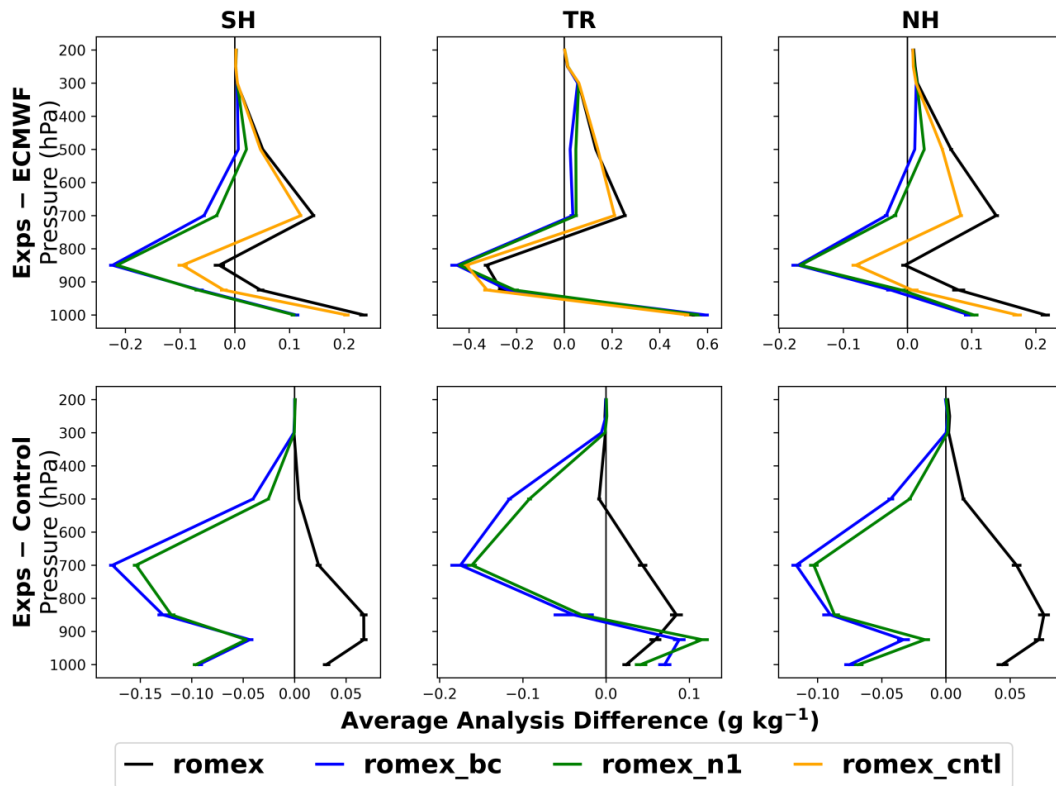


Fig. 9: Same as Fig. 5, but for precipitable water.



305

Fig. 10: Same as Fig. 6, but for specific humidity (unit:  $\text{g kg}^{-1}$ ).



#### 4 Conclusions and Future Work

This study evaluates the impact of assimilating high-volume ROMEX radio occultation (RO) observations on the Navy's global NWP system using a series of observation system experiments. Results show that ROMEX data drive a large impact on the resulting analyses and forecasts. In general, the ROMEX data provide beneficial contributions to forecast skill. A small but consistent bias in the innovations, particularly in the 10-35 km region, was found through the early stages of the ROMEX collaborative experiment. We examined two approaches to address this: an empirical bias correction developed using all ROMEX observations and innovation statistics, and an adjustment to the refractivity coefficient.

In particular, the fit-to-observations against global radiosondes shows improvements for all experiments using the ROMEX data for temperature (100–400 hPa), pseudo–relative humidity (400–925 hPa), and upper-level winds, with the experiments using either bias treatment (`romex_bc`) or adjustment of the refractivity coefficient (`romex_n1`) yielding the largest overall improvements. The forecast sensitivity to observation impact further confirms that all the RO missions in the ROMEX data contribute positively to reducing 24-h forecast error. The Spire missions, which provide the largest volume of RO measurements, show the greatest total impact, while the COSMIC-2 mission consistently shows the highest per-observation effectiveness in the NAVDAS-AR and NAVGEM system.

The standard romex experiment amplifies existing NAVGEM analysis biases in geopotential height and temperature, while reducing a free-tropospheric moisture dry bias. Applying empirical bias correction to the observation (`romex_bc`) or adjusting refractivity coefficient for RO forward operator (`romex_n1`) substantially reduces these geopotential height and temperature biases and improves forecasts of these variables as well. Overall, a change in the treatment of the observations was key to realizing the forecast benefits of massive increase of RO observation provided through the ROMEX data.

Future work will focus on identifying the sources of persistent biases and improving the representation of RO observations in the data assimilation system. In particular, further investigation is needed to better characterize observation and representativeness errors in the lower troposphere and to evaluate alternative strategies within the forward operator and observation processing. Additional studies will also examine the impact of ROMEX data under different observing system configurations and model resolutions, as well as their role in improving forecasts of specific weather phenomena.

#### Code, data, or code and data availability

ROMEX data are available for scientific studies. Users of ROMEX data are required to sign a data license with EUMETSAT for the terms and conditions of using the data (<https://rowg.org/ro-modeling-experiment-romex/>). Other baseline data used in the operational NAVGEM are publicly available through the World Meteorological Organization Global Telecommunications System. Users can access the data from many operational centers (e.g., <https://nomads.ncep.noaa.gov/pub/data/nccf/com/gfs/prod/>). NAVGEM software is considered sensitive intellectual property, therefore is not accessible to the public or research community.

#### Author contributions

HWC conducted the experiments, performed the data analysis, and led the manuscript writing. BR contributed to the experimental design. DT facilitated the license agreement with NRL legal and acquired the ROMEX dataset for this study. All authors reviewed, edited, and approved the final manuscript.



### Competing interests

At least one of the (co-)authors serves as editor for the special issue to which this paper belongs.

### Acknowledgements

345 The authors acknowledge the Navy's high-performance computing resources and funding support from the Office of Naval Research (Awards N0001423WX00473, N0001424WX00933, N0001425GI02277 under Program Element 0603207N).

### References

- Anthes R. A., C. M., Benjamin Ruston, and Hui Shao, 2024: Radio Occultation Modeling Experiment (ROMEX): Determining the Impact of Radio Occultation Observations on Numerical Weather Prediction. *Bull. Am. Meteor. Soc.*: E1552–E1568.
- 350 Aparicio, J., and G. Deblonde, 2008: Impact of the assimilation of CHAMP refractivity profiles in Environment Canada global forecasts. *Mon. Wea. Rev.*, 136, 257–275, <https://doi.org/10.1175/2007MWR1951.1>.
- Bowler N. E., H. Zhang, H. Anlauf, J. M. Aparicio, H. Christophersen, E-H. Kim, X. Li, Y. Liu, K. Lonitz, Y. Murakami, D. Raspaud, B. Ruston, 20026: Inter-comparison of GNSS-RO quality control checks in NWP Part I: survey of methods. *Wea. Forecasting*, accepted.
- 355 Baker N., Rosmond T., Hoppel K., P. Pauley, B. Ruston, and S. Swadley, 2017: The assimilation of water vapor information from satellite observations and the choice of the analysis variable. 17th Conference on Satellite Meteorology and Oceanography. Annapolis, MD.
- Bowler N. E., Hailing Zhang, Harald Anlauf, Josep M. Aparicio, Hui Christophersen, Eun-Hee Kim, Xuanli Li, Yan Liuh, Katrin Lonitz, Yasutaka Murakami, Dominique Raspaud, Benjamin Ruston, 2026: Inter-comparison of GNSS-RO quality control checks in NWP Part I: survey of methods, *Wea. Forecasting*, accepted.
- 360 Christophersen, H., Ruston, B., and Baker N. L., 2023: Assimilation of GNSS Zenith Total Delay in NAVGEM. *J. Geophys. Res. Atmos.*, 1-17.
- Cucurull, L., and J. Derber, 2008: Operational implementation of COSMIC observations into the NCEP's Global Data Assimilation System. *Wea. Forecasting*, 23, 702–711, <https://doi.org/10.1175/2008WAF2007070.1>.
- 365 Cucurull, L., R. Atlas, R. Li, M. Mueller, and R. Hoffman, 2018: An observing system simulation experiment with a constellation of radio occultation satellites. *Mon. Wea. Rev.*, 146, 4247–4259, <https://doi.org/10.1175/MWR-D-18-0089.1>.
- Culverwell, I. D., Lewis, H. W., Offiler, D., Marquardt, C., & Burrows, C. P. ,2015: The Radio Occultation Processing Package, ROPP. *Atmospheric Measurement Techniques*, 8(4), 1887–1899. <https://doi.org/10.5194/amt-8-1887-2015>
- Daley, R., & Barker, E., 2000: NRL Atmospheric Variational Data Assimilation System (163 pp.). Retrieved from <https://apps.dtic.mil/sti/citations/ADA383797>
- 370 Dee, D. P., & Da Silva, A. M., 2003: The choice of variable for atmospheric moisture analysis. *Mon. Wea. Rev.*, 131(1), 155–171. [https://doi.org/10.1175/1520-0493\(2003\)131<0155:TCOVFA>2.0.CO;2](https://doi.org/10.1175/1520-0493(2003)131<0155:TCOVFA>2.0.CO;2)
- Duncan, D. I., Bormann N., A.J. Geer, and P. Weston, 2022: Assimilation of AMSU-A in All-Sky Conditions. *Mon. Wea. Rev.*, 150(5): 1023-1041.
- 375 Frolov S., W. Campbell, B. Ruston, C. H. Bishop, D. Kuhl, M. Flatau, and J. McLay, 2020: Assimilation of Low-Peaking Satellite Observations Using the Coupled Interface Framework. *Mon. Wea. Rev.*, 148, 637-654.



- Healy, S., and J.-N. Thépaut, 2006: Assimilation experiments with CHAMP GPS radio occultation measurements. *Quart. J. Roy. Meteor. Soc.*, 132, 605–623, <https://doi.org/10.1256/qj.04.182>.
- Hogan, T. F., Liu, M., Ridout, J., Peng, M., Whitcomb, T., Ruston, B., et al. (2014). The Navy Global Environmental Model. *Oceanography*, 27(3), 116–125. <https://doi.org/10.5670/oceanog.2014.73>
- 380
- Kursinski E. R., G. A. H., J. T. Schofield, R. P. Linfield, K. R. Hardy, 1997: Observing Earth's atmosphere with radio occultation measurements using the Global Positioning System. *J. Geophys. Res. Atmos.*, 102: 23429 - 23465.
- Privé, N. C., R. M. Errico, and A. E. Akkraoui, 2022: Investigation of the potential saturation of information for the Global Navigation Satellite System radio occultation observations with an observing system simulation experiment. *Mon. Wea. Rev.*, 150, 1293–1316, <https://doi.org/10.1175/MWR-D-21-0230.1>.
- 385
- Rosmond, T., & Xu, L. (2006). Development of NAVDAS-AR: Non-linear formulation and outer loop tests. *Tellus, Series A: Dynamic Meteorology and Oceanography*, 58(1), 45–58. <https://doi.org/10.1111/j.1600-0870.2006.00148.x>
- Ruston B. and S. Healy, 2020: Forecast Impact of FORMOSAT-7/COSMIC-2 GNSS Radio Occultation Measurements. *Atmospheric Science Letters*. DOI: 10.1002/asl.1019.
- 390
- Smith, E., & Weintraub, S., 1953: The constants in the equation for atmospheric refractive index at radio frequencies. *Proceedings of the IRE*, 41(8), 1035–1037. <https://doi.org/10.1109/jrproc.1953.274297>
- Stone, R. E., Reynolds, C. A., Doyle, J. D., Langland, R. H., Baker, N. L., Lavers, D. A., & Ralph, F. M. (2020). Atmospheric river reconnaissance observation impact in the Navy global forecast system. *Mon. Wea. Rev.*, 148(2), 763–782. <https://doi.org/10.1175/MWR-D-19-0101.1>
- 395
- Wilks, D. S., 2011: *Statistical Methods in the Atmospheric Sciences*. Academic Press, 676 pp.